Colloquium: Femtosecond x-ray crystallography

Antoine Rousse

Laboratoire d'Optique Appliquée, ENSTA/Ecole Polytechnique, UMR 7639 CNRS, Chemin de la Hunière, F-91761 Palaiseau, France

Christian Rischel

Department of Mathematics and Physics, Royal Veterinary and Agricultural University, Thorvaldsensvej 40, DK-1871 Frederiksberg C, Denmark and Niels Bohr Institute, Blegdamsvej 17, DK-2100 Copenhagen, Denmark

Jean-Claude Gauthier

Laboratoire pour l'Utilisation des Lasers Intense, Ecole Polytechnique, UMR 7605 CNRS, F-91128 Palaiseau, France

(Published 2 January 2001)

This article gives an overview of recent x-ray diffraction experiments with time resolutions down to 10^{-13} s. The scientific motivation behind the development is outlined, using examples from solid state physics and biology. The ultrafast resolution may be provided either by fast detectors or short x-ray pulses, and the limitations of both techniques are discussed on the basis of state of the art experiments. In particular, it is shown that with present designs, high time resolution reduces the structural information attainable with high spatial resolution, thereby limiting feasible experiments on the ultrashort time-scale. The first experiment showing subpicosecond conformation changes was recently achieved with simple solids using an ultrafast laser-produced plasma x-ray source. The principles of this experiment are described in detail.

CONTENTS

I. WHY?

Time-resolved experiments are used to monitor time-dependent phenomena. From the simplest visual observation of evolving reactions, time-resolved studies have developed in two directions: ever higher time resolution, in order to investigate faster processes, and ever more powerful diagnostics, in order to give an increasingly detailed picture of intermediates. For processes governed by atomic motions—including most of biology and chemistry, and a good part of physics—the shortest time of interest is the duration of one vibrational period, typically 10^{-13} s or 100 fs. In the detailed characterization of structure on the atomic level x-ray diffraction is an unparalleled tool, perhaps most impressive in the mapping of biological structures. Thus one might say that characterization of reaction intermediates by x-ray diffraction with femtosecond time resolution is the ultimate time-resolved experiment. In this article we describe the work towards this goal at our laboratory and others, and we outline its future development as we see it.

A. The femtosecond realm

The time scale of a few picoseconds forms a boundary between two distinct types of reaction dynamics. Slower processes, with characteristic times from nanoseconds to years, are governed by random diffusion of atoms and molecules. Often they are *activated*: the intermediates occupy conformations around local minima on the potential-energy surface with a Boltzmann distribution, and the reaction rate is determined by the faint probability of attaining the conformation with the highest energy on the path to the next, deeper minimum. The first direct demonstration of a qualitatively different domain of chemical reactions was probably that of Zewail and co-workers (Williamson *et al.*, 1992; Williamson and Zewail, 1994; Zewail, 1996), who observed long-lived coherent vibrations in excited diatomic and triatomic molecules. Surprisingly, the same phenomena were observed in proteins in solution (Vos *et al.*, 1991, 1993), showing that vibrational relaxation in complex molecules is much slower than previously thought. These

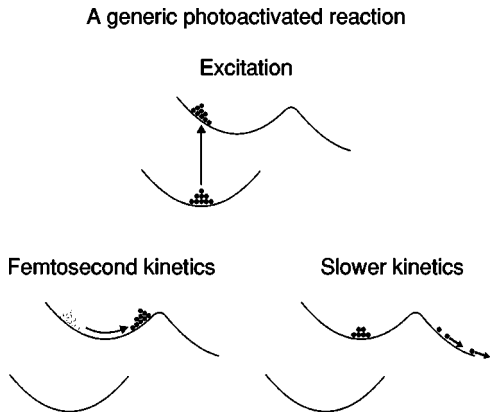

FIG. 1. Subpicosecond reactions versus slower reactions.

results are examples of deterministic reaction dynamics, in which the atoms in the sample move on the potential-energy surface without any dephasing phenomena, rather than being governed by a Boltzmann distribution. Figure 1 sketches the difference between the slow, stochastic regime and the deterministic subpicosecond regime.

In solids, long-wavelength acoustic vibrations can persist for seconds or longer, but oscillations with wavelengths down at the atomic scale generally relax in a few ps. The ultrafast melting of laser-heated crystals deduced from optical probe measurements (Shank *et al.*, 1983a, 1983b; Shumay and Höfer, 1996; Sokolowski-Tinten *et al.*, 1991, 1995, 1998) is an example of a process in a solid taking place much faster than thermal equilibration. Recent measurements on laser-heated GaAs (Glezer *et al.*, 1995a, 1995b; Huang *et al.*, 1998) show that the description in terms of a (hot) temperature is only appropriate several picoseconds after excitation. These concurrent observations in quite different systems show that structural measurements with time resolution of a picosecond or less should be particularly interesting, since we can expect to trap highly reactive states before thermal fluctuations have had the time to blur the atomic positions.

B. The power of x rays

Time-resolved experiments with subpicosecond time resolution have been performed for about 15 years, with probe wavelengths ranging from the ultraviolet to the infrared. With ultraviolet or visible light, the experimentalist can probe the evolution of the excited electronic states in the sample. This is the quantity of interest for a number of subjects, such as electron-hole dynamics in solids (Othonos, 1998) or excitation transfer in photosynthetic complexes (Liebl *et al.*, 1996) but if the process under study involves structural change, one only receives very indirect tidings. Sometimes partial structural information can be obtained from frequencies of nuclear vibrations, which can be measured by Raman spectroscopy, by infrared absorption spectroscopy, or in coherent oscillations. If a signal can be assigned to a particular vibrational mode, the frequency is a sensitive monitor of the local conformation, although it can be difficult to reliably interpret frequency shifts.

X-ray diffraction has the potential to give a complete, global picture of structural changes, without any ambiguity in the interpretation. The x-ray photons scatter from all the electrons in the sample, so the diffracted intensity depends directly on the electronic density. Since most electrons follow the nuclei, the electronic density closely reflects the atomic structure. Time-resolved x-ray-diffraction experiments with nanosecond time resolution have been used for about 15 years to study structural processes in solids such as annealing, crystallization or shock propagation (Larson *et al.*, 1982, 1983; Lunney *et al.*, 1986; Zigler *et al.*, 1987; Wark *et al.*, 1992; Wark, 1996; Helliwell and Rentzepis, 1997). Very recently, it has become possible also to study changes of the much more complicated biological molecules on the nanosecond time scale by x-ray diffraction (Šrajer *et al.*, 1996; Wulff, Bourgeois, Ursby, *et al.*, 1997; Wulff, Bourgeois, and Schotte, 1997; Perman *et al.*, 1998). The challenge which is presently being addressed is to push the time resolution into the subpicosecond domain.

C. Some experiments to aim for

A great number of ultrafast phenomena in biology, chemistry, and physics have been investigated with optical probes. In this section we discuss some of the reactions to which x-ray crystallographic probing can bring a deeper understanding—and which fulfill the experimental constraints described later in the article. We concentrate on solid-state physics and biology; for descriptions of possible applications in small molecule chemistry we refer to other recent papers (Cao and Wilson, 1999; Cao *et al.*, 1999).

1. Solid-state physics

In basic condensed-matter physics, obvious interests are the nature and characteristic times of atomic rearrangements during phase transitions and the relation between amorphous, liquid, and crystalline states.

Solid to solid transitions can be found in a number of materials. An interesting material is the perovskite $KNbO_3$ which experiences a rhomhedral-orthorhombic-tetragonal-cubic sequence as it is heated (Jona and Chirane, 1962). This crystal exhibits ferroelectricity at a transition temperature called the Curie point (T_c). At this temperature, the local electric field induced by the polarization increases much faster than the elastic recoil leading to an asymmetric atomic displacement and the abrupt appearence of ferroelectricity in the cubic phase. Using Raman spectroscopy, Sokoloff and co-workers demonstrated ten years ago the subpicosecond characteristic time of such transitions (Sokoloff *et al.*, 1988). Nevertheless, the microscopic pathway along which atoms move in the lattice from one phase to another phase is not well understood (Dougherty *et al.*, 1992) because Raman spectroscopy cannot clearly determine the type of transition: displacive or order-disorder. An order-

disorder transition exhibits multiple minima through which atoms tunnel out at T_c. A displacive transition is a shift of the minimum of the potential-energy surface at T_c. If the sample can be heated rapidly with an ultrashort laser pulse, subpicosecond time-resolved x-ray diffraction can possibly provide a quantitative description of the microscopic pathway, giving a clear picture of these ultrafast transient processes.

Ultrafast solid to liquid transitions were first investigated by Shank and co-workers (1983a). They demonstrated that a strong electronic excitation—lasting less than the relaxation time—of a crystalline semiconductor may induce structural instability and ultrafast disordering (melting) of the lattice at a temperature well below the one required for thermal melting. Femtosecond reflectivity measurements on silicon showed that the reflectivity of a liquid state is already reached a few hundreds of a femtosecond after the deposition of the laser energy into the sample, and second harmonic emission analysis indicated an atomic disordering consistent with melting (one generally considers that a solid is melted when the root-mean-square displacement of each atom is a fraction of 0.2 of the dimension of the unit cell: ~1 Å for silicon). Numerous experiments have extended these results to other solids [Au (Fann *et al.*, 1992), GaAs (Saeta *et al.*, 1991; Sokolowski-Tinten *et al.*, 1998; Huang *et al.*, 1998), and InSb (Shumay and Höfer, 1996)]. Recent theoretical and numerical studies of the structural dynamics (Stampfli and Bennemann, 1994, 1995; Graves and Allen, 1999) confirm that the dense electron-hole plasma produced by the intense femtosecond laser pulse produces a destabilization of the lattice. The promotion of 15% of the electrons from bonding to antibonding states induces an average displacement of 1 Å in 120 fs and 200 fs in Si and GaAs, respectively.

The crystal may either recover from the ultrashort laser irradiation or switch to an amorphous phase. Conversely, Solis and co-workers have recently shown that thin films of amorphous GeSb can undergo subpicosecond crystallization when high concentrations of carriers are produced on the femtosecond time scale (Solis *et al.*, 1996, 1998). They have also shown that the crystallization process is significantly enhanced compared to subnanosecond irradiation, making this material a suitable candidate for laser-driven phase change optical recording due to its large optical contrast between amorphous and crystalline phase (Afonso *et al.*, 1996). Ultrafast time-resolved x-ray diffraction may directly probe the instantaneous atomic positions to provide direct experimental investigations of these expected ''cold'' liquid phases and ultrafast crystallization.

2. Ultrafast biology

Many fundamental biological events take place in picoseconds or femtoseconds (Vos and Martin, 1999) so ultrafast biology in principle offers a vast field of study. As we describe in more detail in Sec. II, it is, however, experimentally only possible to study processes that can be initiated by a flash of light, and this is a quite restrictive requirement. The ultrafast structural transitions in biology that have been studied with optical probes fall into two main classes: photoinduced isomerizations and ligand dissociation in heme proteins.

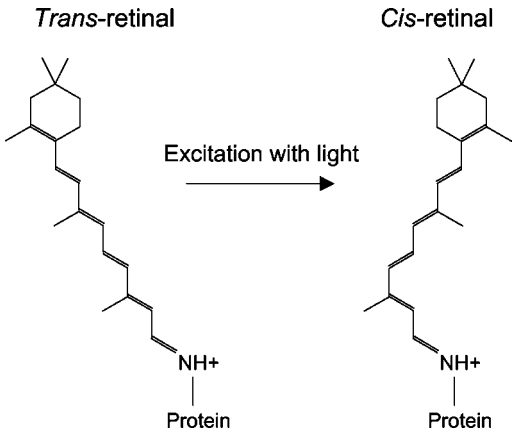

FIG. 2. *Cis-trans* isomerization of retinal. The reaction is coupled to a structural change of the surrounding, much larger protein.

Photoinduced isomerization occurs when absorption of light by some part of a protein molecule creates an excited state which relaxes by rotation of one or more atoms around a chemical bond, switching between *cis* and *trans* isomers (see Fig. 2). One important example is the process of light detection in vision, which is initiated by isomerization of retinal from all-*trans* to 13-*cis* within the protein rhodopsin (Kochendoerfer and Mathies, 1995). The same mechanism in the protein bacteriorhodopsin provides a proton pump necessary for production of ATP in the bacterium *Halobacterium salinarium* (Lanyi, 1997). Determination of the detailed structure of the excited state prior to isomerization as well as of the isomerized state, would provide crucial information on the mechanism. All-optical experiments on bacteriorhodopsin (Gai *et al.*, 1998) show that the excited state develops very rapidly (30 fs), the subsequent *trans-cis* isomerization proceeding on the picosecond time scale and the spontaneous reversion *cis-trans* occurring in about 10 ms. Thus the transient 13-*cis* structure can be determined with the nanosecond experiments that are already working (Šrajer *et al.*, 1996; Perman *et al.*, 1998), but characterization of the excited state is a potential goal for picosecond or femtosecond x-ray diffraction. It should be noted that the x-ray structure of an intermediate state in the bacteriorhodopsin photocycle has been determined by trapping it at low temperatures (Edman *et al.*, 1999). This structure is probably similar to the room-temperature *cis*-intermediate state.

In the bacterial photoactive-yellow-protein light also induces isomerization of an internal chromophore (4-hydroxy cinnamic acid), and the time scales of the subsequent reactions are quite similar to the bacteriorhodopsin case. The biological role of the photoactive yellow protein is not well understood, but the study of the photoisomerization is far advanced: the x-ray structure 1 ns after excitation with a pulse of light was recently determined (Perman *et al.*, 1998). This work pro-

vides a detailed picture of the changes in the interactions with the surrounding protein after photoisomerization; with subpicosecond time resolution one might hope to capture the excited state and to follow directly how the induced strain is relieved in the structural transition.

The heme group is an aromatic molecule that is present in a diverse range of proteins. In some cases, the function of the heme group involves binding of O_2 or NO; it also readily binds CO. Such molecules that may bind are called ligands. The interaction between heme proteins and their ligands has been studied extensively by ultrafast spectroscopy (Vos and Martin, 1999). One important example is hemoglobin, which serves to transport oxygen in the blood, and consists of four subunits with one O_2 binding site in each subunit. It is an essential feature of hemoglobin function that binding of O_2 to one subunit increases the affinity of binding in the other subunits. The transmission of information through the protein has been extensively studied during the last 40 years (Perutz *et al.*, 1998), and is believed to be initiated by the heme changing from a domed structure to a flat one upon ligand binding, triggering large relative movements of the four subunits. When heme with a bound ligand is illuminated with light of the appropriate wavelength, the ligand dissociates. This is not a natural aspect of hemoglobin function, but it allows ligand dissociation to be triggered by an ultrashort light pulse. The subsequent response of the heme group has been probed by ultrafast spectroscopy (Franzen *et al.*, 1995) and the results have been interpreted as showing a heme doming in about 0.5 ps. X-ray diffraction, on the other hand, could detect the details of the response of the surrounding protein, and directly address the central dynamical process whereby a small movement in the heme group is amplified into a large movement in the protein.

Myoglobin, which binds oxygen in muscle tissue, closely resembles one subunit of hemoglobin. From the x-ray structure of myoglobin it is far from obvious how O_2 (or CO or NO) can move between the heme and the exterior through the protein, and this question has been extensively studied by time-resolved spectroscopy on time scales from seconds to femtoseconds (Nienhaus *et al.*, 1997). After dissociation of a bound ligand by a flash of light, the rebinding to the heme can be monitored by absorption spectroscopy. X-ray crystallography can determine the movement of the O_2/CO/NO molecule prior to rebinding, and the response of the entire protein; this has so far been achieved with CO as ligand in nanosecond time-resolved experiments (Teng *et al.*, 1997) and by trapping intermediates at low temperature (Schlichting *et al.*, 1994; Hartmann *et al.*, 1996). These studies localize unbound CO to certain sites within the protein. With picosecond time resolution it should be possible to follow the first parts of the motion after dissociation, and to correlate the response of the protein with the movement of the ligand.

II. HOW?

A. Pump-probe experiments

A time-resolved experiment inherently begins with the initiation of the process under study, at some more or less accurately defined instant in time. The initiation can for instance be done by mixing solutions together or by changing the conditions of the sample (temperature, electric field, etc.). If an optical transition exists to start the process, the initiation can be done with a pulse of light, which is termed the ''pump'' pulse. The subsequent development is then investigated by probing the sample in some way; this sequence constitutes a pump-probe experiment.

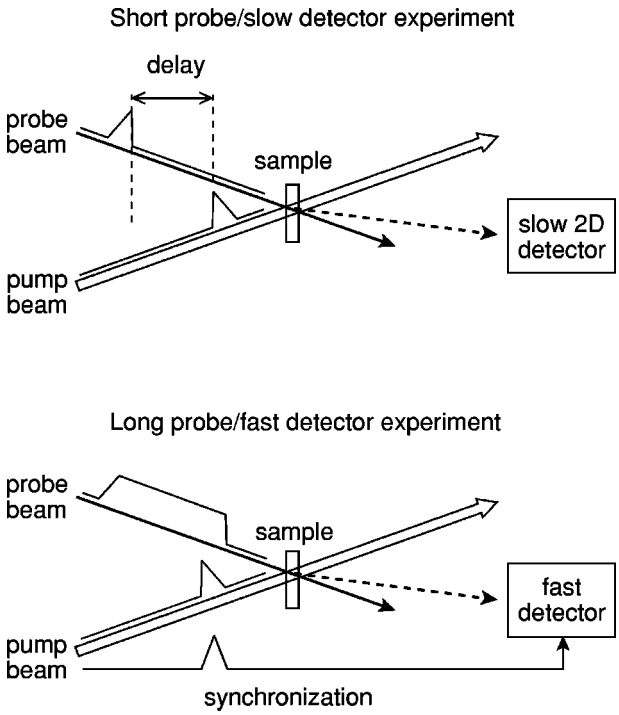

FIG. 3. Two types of pump-probe experiments.

B. Short probe versus fast detector

The time resolution of a pump-probe experiment is, obviously, determined by the duration of the pump as well as the resolution of the probing. Mixing of liquids can be done in as few as 10 μs and switching of electrical fields and currents can be done in about 1 ns. Significantly faster resolution than this can only be obtained with optical pump pulses. Thus the development of ultrafast spectroscopy has closely followed the advances in pulsed laser technology, which presently achieves pulse durations down to about 5 fs (Stingl *et al.*, 1995; Baltuska *et al.*, 1997; Backus *et al.*, 1998). The pump pulse must always be as short as the desired time resolution, but the probe can be temporally resolved in two ways: by having a short probe pulse or by having a fast detector and quasicontinuous probe illumination (see Fig. 3). In the case of a short pulse, the probe pulse follows the pump pulse at some specified delay. The signal recorded by the detector then reflects the state of the sample during the brief probing. The experiment must be repeated many times with different delays in order to reconstruct the full kinetics of the reaction. In the case of a fast detector, the sample is probed continuously and the sig-

nal is resolved temporally by the detector. This permits the entire reaction kinetics to be recorded simultaneously.

In order to achieve a time resolution below 1 ns with a fast detector, one must use streak cameras, in which photoelectrons generated by the probe beam are swept across the detection screen by an electric field ramp. Resolutions down to 0.88 ps have been obtained in that way (Chang *et al.*, 1996; Larsson *et al.*, 1997). Unfortunately, the physics of streak cameras is such that high time resolution is obtained at the expense of sensitivity, a fact that has so far limited the use of this technology. In experiments with an optical probe it is preferred to use a fast probe pulse instead, in particular since a short optical pulse must be available for the pumping in any case. The situation is different in the case of an x-ray probe, since the short x-ray pulses that can presently be made do not have all the desired properties. Both fast detector and short pulse techniques are being developed for ultrafast x-ray-diffraction experiments.

C. Single-shot versus multishot

Another important classification of pump-probe experiments is whether the sample is irreversibly modified by the pump pulse. If this is the case, an exposed sample cannot be used again; this is referred to as a single-shot experiment. In a number of cases, the sample reverts to the initial state, typically after a time that is long compared to the time scale of the pump-probe sequence. As an example, one can think of a crystal heated to a temperature below the melting point. Initially the lattice expands, but after a while the conduction of heat will return the sample to the equilibrium temperature. One can then perform a multishot experiment by repeating the pump-probe sequence over and over again, in order to improve the data.

Even single-shot experiments usually require several shots, for example, several different pump-probe delays, to give meaningful results. Therefore experiments of this type often require appreciable amounts of material, as the sample must be replaced for each new shot. This requirement is particularly restrictive in the case of x-ray diffraction, since single crystals with a size that permits many shots are only available for a quite restrained range of materials. Due to the much weaker diffraction of polycrystalline substances, experiments with such samples presently appear to be very difficult. Multishot experiments, on the other hand, are limited by the requirement that the sample must return to the initial state at some time after the pump pulse. Fortunately, several potential topics of study do benefit from this property. Within the biological applications, it is notably the case for ligand dissociation from heme proteins (Šrajer *et al.*, 1996) and for the structural transitions inside the photoactive yellow protein (Perman *et al.*, 1998). Within the field of condensed-matter physics, certain simple crystals are known to recrystallize after laser-induced surface melting, as discussed in Sec. I.C.1. However, it must be expected that single-shot experiments will be necessary for general studies of the melting process. Whether a sufficient signal can be aquired in single shots depends on the detailed properties of the x-ray source and the sample.

D. X-ray sources

The great potential of ultrafast x-ray techniques has initiated the development of ultrafast x-ray sources and innovative detection systems. The x-ray sources must satisfy particular requirements concerning their pulse duration, spectrum, brightness, and overall photon flux. Among the newer sources of pulsed x rays, we will in this section mainly discuss the characteristics of synchrotron radiation and laser-produced plasma sources, but also briefly mention a number of other candidates.

There are practical difficulties in comparing the relative benefits and drawbacks of these various x-ray sources due to the different requirements of different experiments. We have chosen to compare the sources according to their peak spectral brilliance B_{peak}, expressed as a number of x-ray photons per 100 fs per square millimeter per square milliradian in a spectral bandwidth of 0.1% of the photon energy. This comparison should be taken with some caution. The peak spectral brilliance is proportional to the number of photons emitted by the source divided by the pulse duration, favoring bright and ultrashort pulsed sources. It is not taken into account that long probe pulses permit the entire time course to be recorded in one pulse. However, this advantage is in experiments compensated by the much lower efficiency of fast detectors. Also important in the expression of the peak spectral brilliance is the emittance in the transverse direction (the product of the size of the source and its divergence), which favors small sources with emission in a narrow solid angle. It is generally beneficial to have a small source but there is no advantage in reducing it much below the resolution of the detector system, so the high peak brilliance of very small sources does not translate into an experimental advantage. A similar qualifying remark applies to the importance of the divergence. The experimental repetition rate will in all cases be limited by the pump laser, so we do not consider this parameter.

1. Synchrotron radiation

Here we will concentrate on the performances which will be obtained or which are obtained with third generation storage rings such as the European Synchrotron Radiation Facility (ESRF) in Grenoble. At the ESRF, the x-ray pulse duration is about 150 ps at 15 mA current per bunch. Due to the rather long revolution time ($\sim 3\ \mu s$), it is possible to isolate single x-ray pulses by a rotating wheel (Wulff, Bourgeois, Ursby, *et al.*, 1997). In Fig. 4 is plotted the peak spectral brilliance as a function of photon energy for the ESRF. X rays are emitted from the electrons as they travel through a period magnetic field (a wiggler), which gives a broad and smooth spectrum around 10 keV. With this source, a Laue pattern of broadband x-ray diffraction from MbCO has been re-

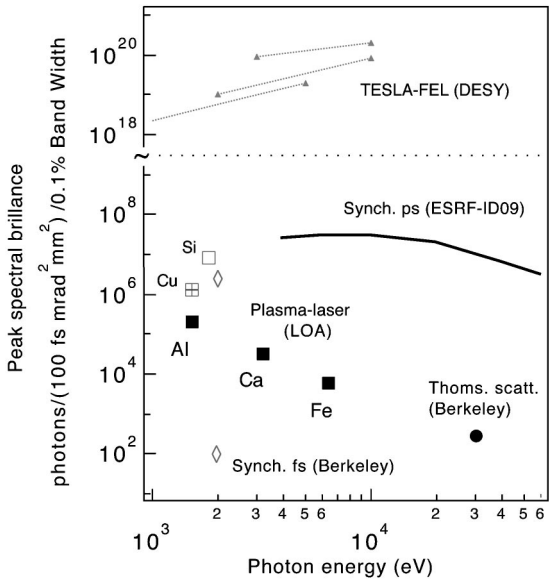

FIG. 4. Peak spectral brilliance in photons/(100 fs mrad^2 mm^2)/(0.1% bandwidth) as a function of photon energy. Solid lines: synchrotron radiation insertion device (ESRF-W70); triangles: x-ray-free electron laser; diamonds: synchrotron radiation from sliced electron bunches; squares: laser plasma K-line radiation; crossed square: laser plasma thermal radiation; circle: Thomson scattering.

corded in a single pulse of 150 ps. The bandwidth was 7–38 keV and the incident polychromatic flux through the sample was 8×10^{10} photons per pulse (Wulff, Bourgeois, Ursby, *et al.*, 1997). Its combination with a nanosecond pump laser has permitted the determination of nanosecond time-resolved protein structures previously mentioned (Šrajer *et al.*, 1996; Perman *et al.*, 1998).

In the context of femtosecond x-ray diffraction, the synchrotron pulse is to be considered a ''long probe,'' so it must be combined with a streak camera in order to achieve the desired resolution. Complete experimental systems with synchronization of pump laser, synchrotron and streak camera have been constructed at the ESRF (Wulff, Bourgeois, Ursby, *et al.*, 1997) and at the Advanced Light Source in Berkeley (Larsson *et al.*, 1997, 1998). The strong point of streak cameras is that a large number of different pump-probe delays are covered. For instance, it is not certain that the coherent acoustic oscillations observed by Lindenberg *et al.* (2000, see Sec. IV.C) would have been discovered if data had been collected for one delay at a time. As already mentioned, the drawback of streak cameras is the low sensitivity, on the order of 0.1%, and their limited signal dynamics, on the order of 20 (i.e., the ratio of the strongest to the weakest detectable signal). This gives a severe drop in the number of detected photons, which means that only multishot experiments can be performed. Further improvements of the source (collimation and divergence) could make this scheme more attractive (the new undulator ESRF-U17 will increase by four orders of magnitude the available peak brilliance).

New experimental techniques to cut a slice of subpicosecond x rays from a single, several tens of picoseconds synchrotron x-ray pulse have recently appeared. In a method developed at the ALS (Zholents and Zolotorev, 1996; Schoenlein *et al.*, 2000), where the x-ray pulse duration is 30 ps, slicing of the long electron bunch is accomplished through the interaction of a femtosecond laser pulse with the electron bunch as they propagate through a wiggler. The high electric field in the optical pulse produces an energy modulation of the electrons of several tens of MeV as compared to the ring energy of 1.5 GeV. Electrons are accelerated or decelerated according to their phase relative to that of the optical pulse. Spatial separation of the ponderomotively scattered electrons from the original bunch is performed in a dispersive (magnet) section of the accelerator and radial apertures. Femtosecond ''dark'' (due to a hole in the electron bunch) and ''bright'' pulsed x rays can be obtained, with a time duration comparable to the optical pulse time length. A significant increase of the peak brilliance is proposed at the ALS with the use of an undulator (see Fig. 4).

2. Laser-produced plasma sources

The study of laser-plasma x-ray emission has been stimulated by the field of laser fusion (Lindl, 1995). Recently, the extension of laser-plasma x-ray sources into the ultrafast, subpicosecond domain have been intricately tied to the progress of laser technology (Perry and Mourou, 1994; Chambaret *et al.*, 1996; Mourou *et al.* 1998; Brabec and Krausz, 2000). Laser-plasmas have a number of characteristics (Murnane *et al.*, 1991; Kieffer *et al.*, 1993, 1996; Rousse *et al.*, 1994) that make them valuable as x-ray sources in time-resolved x-ray-diffraction and -absorption experiments: (i) they can provide a wide range of pulse durations, from a few hundred femtoseconds to hundreds of nanoseconds; (ii) bright x-ray sources can be generated with source sizes as small as a few microns; and (iii) laser-plasma x-ray sources can be accurately synchronized with other events that can be driven, triggered, or stimulated by the same laser light.

When a high intensity laser is focused onto a solid, the target absorbs laser energy over a very short distance ($\sim$10 nm). In the heated region, the electron temperature can reach values of 100–1000 eV depending on laser intensity. At these high temperatures, thermal x rays at energies above a kilovolt are produced. In addition, nonlinear mechanisms produce fast electrons which give rise to bremsstrahlung and K_α radiation from the target bulk. This emission is thought to be very short because, in principle, fast electrons are produced only during the laser pulse. The fast electrons have proved to be a convenient way of generating x rays in the photon energy range above one keV (Rousse *et al.*, 1994; Bastiani *et al.*, 1997; Gauthier, Geindre, *et al.*, 1997, Gauthier, Bastiani, *et al.*, 1997). In the 1–10 keV energy range, efficient production of K_α radiation in aluminum, calcium, and iron has been demonstrated (Rousse *et al.*, 1994). Results are

shown in Fig. 4 (filled squares) for the three target materials, and it is seen that peak brilliance compares well with synchrotron radiation. The measured source diameter is about 10 μm, the repetition rate is 10 Hz, and the total number of x-ray photons per shot is about 3×10^8.

More recently, we have used a prepulse technique in order to tailor the shape of the electron density gradient at the target surface for optimizing laser absorption by fast electrons (Gauthier, Bastiani, *et al.*, 1997; Bastiani *et al.*, 1997). Increasing the laser energy to 15 mJ and adjusting the delay of the prepulse with respect to the main pulse (prepulse to pulse contrast ratio in intensity is $\sim$0.01), we obtained a photon yield increased by a factor of 40 as compared to the previous results (Rousse *et al.*, 1994) for a silicon target with K_α emission at 7.13 Å. In the experiment to be described below, we refocused the emitted Si K_α radiation by a toroidally bent quartz crystal (100 orientation) of 6×25 mm^2 lateral dimensions. This gives about 5×10^4 photons per shot on the sample over a bandwidth of only $\sim$2 eV. Our most recent experiments show that the duration of the x-ray pulse is less than 300 fs (unpublished results). The range of available x-ray photon energy has been extended to above 8 keV by using 30-fs laser pulses with an average power of 1.5 W; about 2.5×10^8 photons/rad^2/pulse have been produced (Guo *et al.*, 1997). Ten times more powerful ultrafast lasers working at 10 Hz are now available (Chambaret *et al.*, 1996) and should give a tenfold increase in photon number.

The divergence of the plasma sources is not purely a drawback. In the case of crystals with a lattice constant much larger than the x-ray wavelength, it permits many different Bragg reflections to be recorded simultaneously (see Sec. III.B). For a single Bragg reflection, one measures simultaneously the diffracted intensity as function of angle—the rocking curve—over a large angular interval. This gives information about spatial variations of the atomic order (see Sec. III.A). Thus these sources are well suited for obtaining detailed structural information.

3. Other sources

The great potential of ultrafast x-ray techniques is one of the major arguments to build hard x-ray free electron lasers using the SASE (self-amplified spontaneous emission) scheme. X-ray collimated beams (few μrad) as bright as 10^{13} photons/pulse/0.1% bandwidth are expected to be produced at a wavelength of 1 Å in 100 fs (Wiik, 1997). The colossal increase in peak brilliance (see Fig. 4) will completely revolutionize the field, since it will make single-shot experiments on polycrystalline samples possible. The demonstration that x-ray free electron laser systems are able to produce femtosecond x-ray beams is scheduled to take at least ten years (Wiik, 1997).

To overcome the current limits of the third generation of synchrotrons, another approach is coming into light using ultrahigh intensity laser systems. While a synchrotron x-ray source is based on high-energy electron storage rings and undulator magnetic fields, the laser beam could act on the relativistic electron beam as an electromagnetic wiggler with a period 10^5 times shorter than the magnetic undulator. That means that a laser synchrotron source could produce more energetic x-ray photons with the current synchrotron electron beam as well as use 100 times less energetic electrons beams to generate x rays at a particular wavelength. Compactness of such systems will thus be considerably improved, which makes it very attractive for the wide-ranging applications of such x-ray bursts. In addition, one can take advantage of the development of the high-brightness RF linear accelerators (Chan *et al.*, 1998) or the laser-produced plasmas to produce high density picosecond electron bunches (Modena *et al.*, 1995; Esarey *et al.*, 1996).

A completely different approach is to use reversible structural transitions below the damage threshold of solids (Sec. I.C.1) to modulate a diffracted synchrotron beam (Larsson *et al.*, 1998). By combining two crystals in series and varying the time delay between the optical perturbating pulses, a slice of x-ray radiation could be cut. A more appealing technique to modulate long x-ray pulses relies on the scattering of x-ray photons by a superlattice of optical phonons coherently generated by ultrafast laser pulses incident on a Bragg crystal (Bucksbaum *et al.*, 1999). Coherent excitation of phonons and their effects on diffraction efficiency in an InSb (111) crystal has been recently studied (Lindenberg *et al.*, 2000). In coherent phonon x-ray switching, the crystal lattice motion can be controlled so that efficient Bragg diffraction is switched on and off in a time comparable to a phonon oscillation period. Coherent phonon Bragg peaks of 1–10% of the main diffraction peak and switching times in the subpicosecond regime have been predicted (Bucksbaum *et al.*, 1999).

Schoenlein and co-workers at the ALS have produced x-ray pulses just 300 fs long at a wavelength of 0.4 Å (Schoenlein *et al.*, 1996) by directing 100 fs pulses from a terawatt laser across a relativistic electron beam (50 MeV) at a 90° angle, with the laser and electron beam both focused at the intersection point. The photons scatter off the electrons by Thomson scattering, and are energy boosted into the hard x-ray range by relativistic effects. The transit time of the light through the beam determines the length of the scattered light pulse. The number of photons per pulse is about 10^5 and the peak brilliance is quite low, as shown in Fig. 4. A single experiment has been performed with this source (Chin *et al.*, 1999), which has now been abandoned.

Picosecond x-ray pulses can be generated by vacuum diodes operating in transient mode. In this mode, the cathode is triggered by a short light pulse, the duration of which is smaller than the transit time of the electrons in the diode gap. The number of photons emitted increases with the applied voltage. Photon energies are in the 10–100-keV range. The main limitation in obtaining high-power short-pulse duration is due to the temporal dispersion of short electron pulses in the diode in the

space charge regime of operation. Operation of the x-ray diode at the space charge limit could make feasible the generation of x-ray pulses at durations in the range 1–10 ps (Tomov *et al.*, 1997). The repetition rate of these sources may be quite large, up to kHz, but the number of photons per steradian is limited to the range 10^5–10^6, and the source size is millimetric.

III. WHAT?

Ultrafast crystallography is in its infancy, and the experimental constraints still play a dominant role in the choice of samples. In this section we give a somewhat technical discussion of some of the design considerations for different kinds of experiments.

A. Simple solids

The first application of femtosecond time-resolved x-ray diffraction among the potential scientific fields has been the study of ultrafast structural dynamics in condensed-matter physics.

However, what information might we really obtain with such a tool? One has in mind the extremely high quality of crystalline structure analysis developed from the Bragg theory. Qualitative identification of chemical compounds, analysis of crystalline mixtures, and precision determination of lattice constants are all of great importance for solid-state investigations. To fully determine complex crystalline structures with high resolution (a few 10^{-3} Å) requires the recording of a few thousand Bragg reflections. Moderate resolution (a few 10^{-2} Å) still requires hundreds of Bragg reflections, while mere knowledge of the unit-cell size requires fewer than ten Bragg reflections with poor spatial resolution.

It is in principle possible to measure a considerable number of Bragg reflections (giving a high quality of ultrafast transient structural information) if we consider the repetition rate of common laser systems—10 Hz—from which the femtosecond x-ray source is produced. As has been discussed already in this paper, accumulation may be used if the sample recombines to its initial state between consecutive shots and the temperature increase of the sample is controlled to avoid its thermal destruction. Requirements for detecting Bragg reflections are established from the x-ray source flux, the Bragg law (the x-ray wavelength must remain smaller than two times the distance between lattice planes) and the range of integrated reflectivities of useful reflections. As an example, one can consider the ferroelectric phase transition in the perovskite $LaAlO_3$, which might be completed in less than one picosecond. Eight minutes at 10 Hz will be necessary to obtain a reasonable level of 10^2 reflected x-ray photons onto the detector for the hundredth strongest Bragg reflection, so the accumulation time is not limiting. Unfortunately, the combination of an ultrafast x-ray time-resolved experimental setup with the data acquisition techniques used in Bragg crystallography is problematic. All reflections must be measured under identical pumping conditions, so the orientation of the pump beam relative to the sample should be kept constant. At the same time, the angle between pump and probe beams should remain low in order to avoid so-called temporal walk-off (i.e., the mismatch of the temporal superposition between the two beams on the sample). These requirements only allow a limited range of sample orientations, so the state of the art in ultrafast x-ray diffraction does not readily permit high precision experiments. New x-ray-diffraction geometries are required (see Sec. III.B).

In the present experiments only one Bragg reflection can be analyzed. Nevertheless, the spatial information obtained is still of great importance in a number of feasible solid-state physics experiments, such as the study of phase transitions, as discussed in Sec. I.C.1. In experiments with divergent sources (plasmas), the entire rocking curve can be measured at the same time, and it contains much information on the state of the lattice. Figure 5 shows a sketch of a lattice with the different generic changes and the corresponding rocking curves.[1] An *expansion or contraction* of the lattice changes the lattice spacing d. Expansion typically arises as a response to heating; compression can occur if the sample is subjected to a shock wave. The change in d gives a shift in angle of the rocking curve. If there is *inhomogeneity in the lattice spacing*, such that some layers are expanded and others compressed, the result is a broader rocking curve. In the (idealized) event that the average lattice constant remains constant, the midpoint angle of the rocking curve does not change. Finally, *disorder within each layer* results in a decrease in overall intensity. In many instances a complex mixture of these idealized cases will be observed; it is then possible to model the profiles of strain and disorder in the sample (Larsson *et al.*, 1997, 1998; Siders *et al.*, 1999; Rose-Petruck *et al.*, 1999; Lindenberg *et al.*, 2000).

B. Ultrafast protein crystallography

The potentially most rewarding, but also most demanding application of femtosecond x-ray diffraction is the characterization of ultrafast structural processes in biological molecules. From a time-resolved measurement of single-crystal diffraction intensities, the transient changes in electron density of the constituent molecules can be calculated, giving a superbly clear picture of the ultrafast biological reactions. However, in order to determine the electronic density in such large molecules, the intensity of 10^4 or more different diffraction spots must determined. With only one diffracted photon detected per 10^5 incident on the sample, and a reasonable minimum of 10^2–10^3 photons in each spot, it is necessary to put at least 10^{11}–10^{12} photons on the sample in order to perform an experiment.

[1]We only deal with the case where absorption of x rays in the sample dominates over extinction by diffraction. In the opposite limit additional effects can appear.

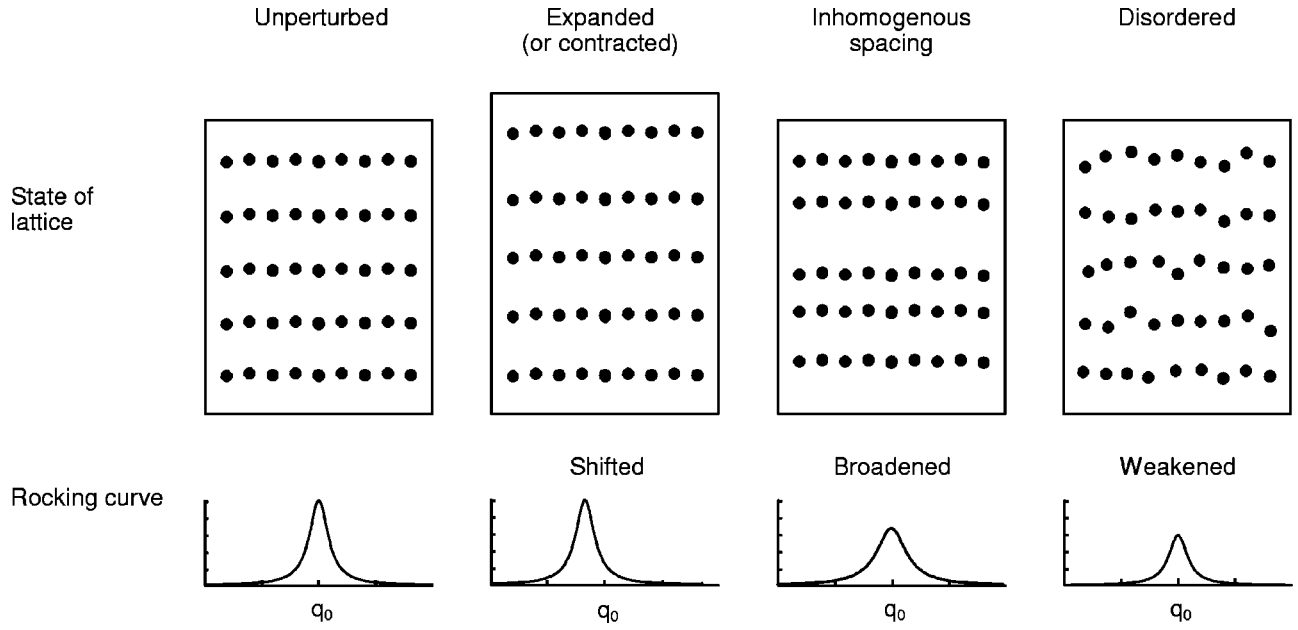

FIG. 5. Different types of transient distortions and their effects on the rocking curve.

Synchrotron sources can in a single pulse of about 150 ps duration deliver a sufficient number of photons to make single-shot experiments possible. For the much weaker femtosecond x-ray sources the situation is quite different, and it will be necessary to accumulate over many shots, so only multishot samples can be used. Repetition rates of 10 or 20 Hz are common for intense femtosecond lasers, while the system at the ESRF has a maximum frequency of 900 Hz. In experiments, the upper limit to the useful rate will be set by the maximum permitted value of the heat load from the optical excitation pulses. The energy necessary to dissociate all CO molecules once in a crystal of MbCO heats the crystal by about 2 °C (assuming the heat capacity of water), so efficient cooling will be necessary in order to attain high accumulation rates, even if only a minor fraction of the molecules in the sample are dissociated.

In order to minimize the accumulation time, the number of useful x-ray photons per shot must be carefully optimized. To this end, we have reconsidered the diffraction geometry in the case of a small and monochromatic, but divergent source, such as a laser-generated plasma. In usual diffraction experiments, a collimated beam is always used. For the case of a collimated beam incident on a single crystal, the experimentalist must either use a monochromatic beam and oscillate the crystal over some angle (Bragg method) or use a polychromatic beam with a stationary crystal (Laue method), in order to pick up the many reflections in a diffraction image. Instead, we have looked at divergent beam methods, which combine a stationary single crystal with a converging or diverging beam. A converging beam results if wide-angle x-ray optics are used to collect the emission from the source and focus it on the sample. Alternatively, one might place the sample close to the source, such that the crystal is directly hit by a diverging cone or fan of photons, covering an appreciable solid angle. In both cases the multitude of directions of the incoming x rays ensures that there are a number of reflections possible.

In Fig. 6 we sketch the different geometries, and show the predicted positions of the reflections from a triclinic

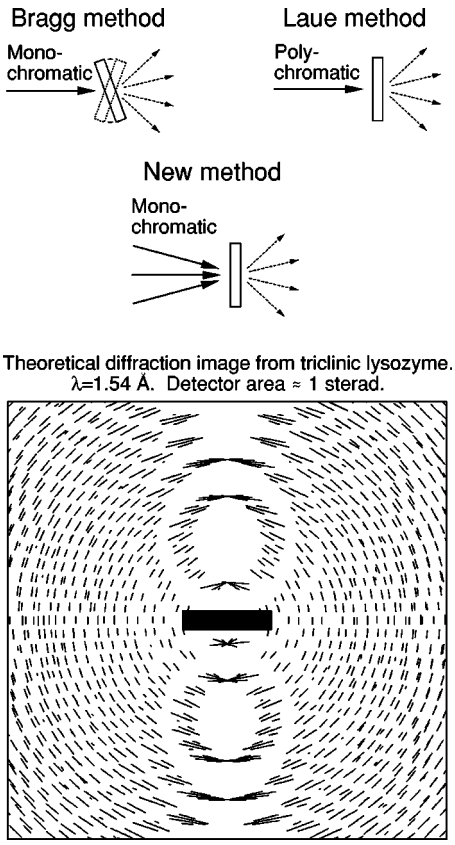

FIG. 6. Different geometries for protein x-ray crystallography (top) and predicted diffraction image from a crystal of triclinic lysozyme in convergent/divergent geometry (bottom).

crystal of the protein lysozyme, illuminated with a 20 $\times$100-mrad^2 fan of Cu-K_α x rays. The fact that each reflection gives rise to a small line on the image can be understood by comparing with the Bragg method. In that case, one obtains point reflections by rocking the crystal back and forth in one dimension. With the divergent beam method, a flat fan of x rays would give the same result, but with a finite thickness of the fan the point spreads to an arc, known as a Kossel line (Galdecka, 1995). It is seen from Fig. 6 that the vast majority of the reflections give well separated signals, with only a small fraction of the lines overlapping; this means that almost all the photons within the fan are useful for the diffraction experiment. With a source intensity of 2 $\times 10^9$ photons/rad^2/shot, one can then put 4×10^6 useful photons on the sample in each shot. To reach a total of 10^{11} photons, 2.5×10^4 shots are necessary; at 10 Hz this takes 42 min. 10^{12} photons are reached in 7 h of acquisition. These estimates show that the x-ray flux necessary for ultrafast protein crystallography can be obtained from laser-generated plasmas. However, it is not yet clear if a sufficient number of different reflections can be collected, given the constraints on the geometry discussed in the previous section (III.A).

With streak cameras, one detects the signals passing through a slit. Therefore, only one or a few reflections can be monitored at a time, but for these reflections a time course of many picoseconds is covered, by the sweep of the slit across the detector. Wulff, Bourgeois, Ursby, *et al.* (1997) have proposed to concentrate on specific locations in the molecule under study, such as the position of the CO bound to myoglobin, and use a limited number of reflections to deduce the electronic density at this particular position after photodissociation of CO. Such a strategy could also be employed for experiments using plasma sources.

C. The pump problem

The restrictive conditions on the samples in multishot experiments have already been discussed. The sample requirements for x-ray diffraction introduce new problems. The high concentration of molecules in the crystal means that, in order to excite a significant fraction of the sample, the pump intensity must be so high that the threshold for irreversible damage is approached.

Damage of a solid by a laser beam can either occur at the surface or by autofocusing of the beam inside the bulk volume, but for crystals with a thickness of a few hundred microns the latter possibility can probably be disregarded. The threshold for surface damage is dependent on the material: for conductors the value is about 0.2 J/cm^2 with pulses of 100 fs (Pronko *et al.*, 1995; Stuart, Feit, Herman, *et al.*, 1996), while a value around 2 J/cm^2 has been inferred for fused silica (Stuart *et al.*, 1995; Stuart, Feit, Herman, *et al.*, 1996; Stuart, Feit, Rubenchik, *et al.*, 1996). For comparison, the excitation of all molecules in a 200-μm-thick crystal of myoglobin, with a concentration of 50 mM, would require an energy of 0.2 J/cm^2 using 2-eV (620-nm) photons. It is improbable that the protein crystal can sustain this intensity for many shots, so it will be necessary to dissociate only a fraction of the molecules in the samples. Experimental determination of these damage thresholds are much needed. For solids, where the concentration is higher yet, the problem is in principle even worse. However, the x-ray probe depth is often only a few microns, due to the presence of heavier elements, so it is only necessary to excite a thin layer near the surface.

When one considers the number of molecules in a biological sample that can be excited by an intense ultrashort pulse, it is important to realize that the Lambert-Beer law, which predicts exponential attenuation of the intensity inside the sample, is invalid when the pulse duration is shorter than the decay of the excitation. In the ideal case the excited state has no absorption; each molecule can then only absorb one photon, and intense pulses are only slowly attenuated. The fact that the molecules in the crystal are oriented, and therefore can be positioned relative to the polarization of the incoming light, might help to approach these conditions (Makinen and Eaton, 1973; Wulff, Bourgeois, Ursby, *et al.*, 1997). Determination of the transient absorption spectra of crystalline samples will be necessary in order to assess the possibilities in this direction.

The fact that the speed of light inside the sample is different for the visible pump pulse (refractive index $n \sim 1.4$) and for the x rays (refractive index ~ 1) puts a lower limit to the time resolution that can be obtained. Since the synchronization cannot be perfect at the front and at the back of the sample at the same time, the resolution will be broadened by $l(n-1)/c$, where l is the sample thickness and c the speed of light. For a crystal thickness of 200 μm, a broadening of about 250 fs is predicted. Neutze and Hadju have proposed a geometry for use with synchrotron radiation, in which pump and probe beams are perpendicular, and the ultrafast time resolution is obtained by analyzing the intensity variations on the image of the crystal on the detector (Neutze and Hadju, 1997). This geometry in principle resolves the problem of refractive index mismatch; however, the method appears to have several impracticalities, including pumping of the crystal along the long direction.

IV. THE FIRST EXPERIMENTS

Our group recently performed the first time-resolved x-ray-diffraction experiment with subpicosecond time resolution (Rischel *et al.*, 1997). In this section we describe the principles of this experiment in detail and we show the newest results (Rousse *et al.*, 1999). We also briefly review two other recent experiments.

A. Femtosecond x-ray diffraction on organic films

The samples under study are Langmuir-Blodgett films of cadmium arachidate. This fatty acid salt has a polar head group, where the cadmium atom is located, and a long, hydrophobic tail. The Cd arachidate molecules can be deposited on a glass substrate in a multilayer film,

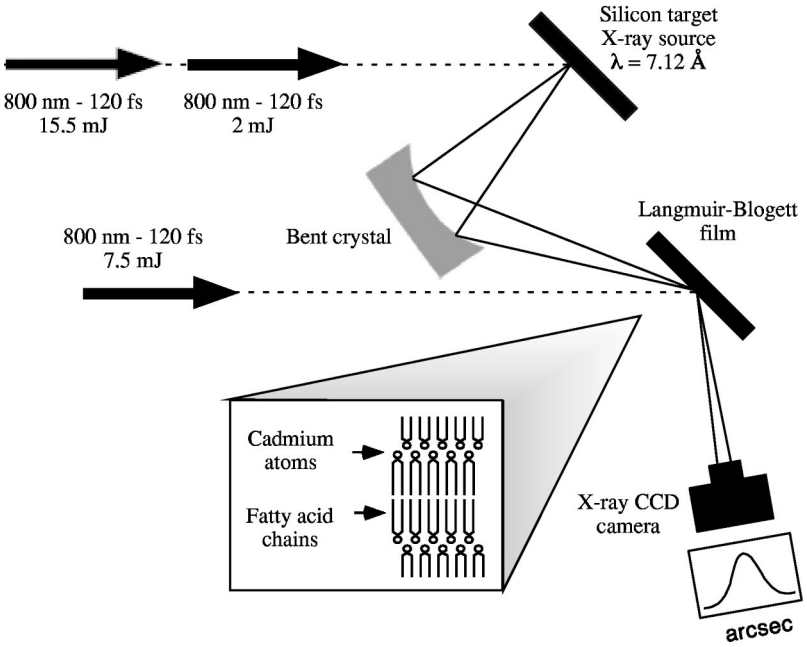

FIG. 7. Sketch of the experimental setup (Rischel *et al.*, 1997).

with alternating orientation of the layers: head group against head group and hydrophobic tail against hydrophobic tail. This places the cadmium atoms in well defined planes with a separation of 55 Å. In our experiment, the film is heated with an ultrashort pulse of infrared light, and the diffraction of an x-ray pulse is used to probe the subsequent evolution of the layered structure. The diffraction of the x rays is almost entirely due to the cadmium atoms, with very little contribution from the fatty acid chains.

A sketch of the experimental setup is shown in Fig. 7. The experiments are performed at the Laboratoire d'Optique Appliquée with a laser facility that delivers 130-fs pulses at 10 Hz, with an energy of 23 mJ at the entrance to the vacuum chamber. The laser beam is split in two: one pulse containing 7.5 mJ heats the sample, the other pulse containing 15.5 mJ is used to generate the x-ray flash. Before entering the vacuum chamber, the x-ray generating pulse is passed through a prepulse system (not shown), which advances the central 10% of the beam by 9 ps relative to the rest of the pulse. Inside the vacuum chamber, the beam is focused on a silicon target. The small prepulse serves to optimize the x-ray yield as described above (Bastiani *et al.*, 1997). The silicon target emits characteristic K_α radiation with a wavelength of 7.12 Å. This is longer than the 0.5–1.5 Å typically used for x-ray diffraction, but well suited for probing the structure of the film, with the relatively large lattice constant. The K_α photons are collected by a toroidally bent crystal of quartz with 100 orientation and focused into a 300-μm-long vertical line on the film. The x rays diffracted from the film are detected by a charge-coupled device camera. The angle between the x rays and the surface of the film is centered at the Bragg angle of 3.7°, and as the toroidal crystal delivers nearly monochromatic radiation over a large horizontal aperture angle, the experiment simultaneously measures the rocking curve in a broad angular interval.

The laser pulse which heats the multilayer film is initially passed through a delay line controlled by a stepper motor (not shown) in order to allow the pump-probe delay to be varied. It is then focused on the film sample with an angle to the surface of 18°. The intensity of the heating can be varied by changing the size of the focal spot. In experiments with intense heating, the spot can only partly cover the x-ray focus, due to the limited laser energy available. One experimental run consists of five shots without the heating pulse (in order to probe the diffraction of the cold surface), one "live" shot with both heating and x-ray pulses, and five more shots without the heating pulse to measure the destruction of the surface. For each value of the delay between the heating and x-ray pulses we make about 20 such runs. The silicon target is moved after each shot to expose a fresh area, and the film is moved after each run.

B. Experimental results

Our first experiments (Rischel *et al.*, 1997) were performed with a pump energy of 15 J/cm^2 with 125-fs pulses, giving an intensity of 1.2×10^{14} W/cm^2. We observed a decrease of the diffracted intensity within a picosecond after the heating pulse, but no shifts of the rocking curve. As explained in Sec. III.A this reveals that the atoms are disordered before the lattice expands or contracts. More recently, we have done the experiment with a lower intensity of 5×10^{13} W/cm^2, where the response of the film is significantly slower. Typical rocking curves are shown in Fig. 8. It is seen that the main effect still is a decrease in the diffracted intensity, with at most a slight shift, corresponding to a small expansion of the lattice. This is markedly different from the results obtained on slower time scales, which all show a clear expansion of the lattice after the heating (Chen *et al.*, 1996; Larsson *et al.*, 1998; Chin *et al.*, 1999; Rose-Petruck

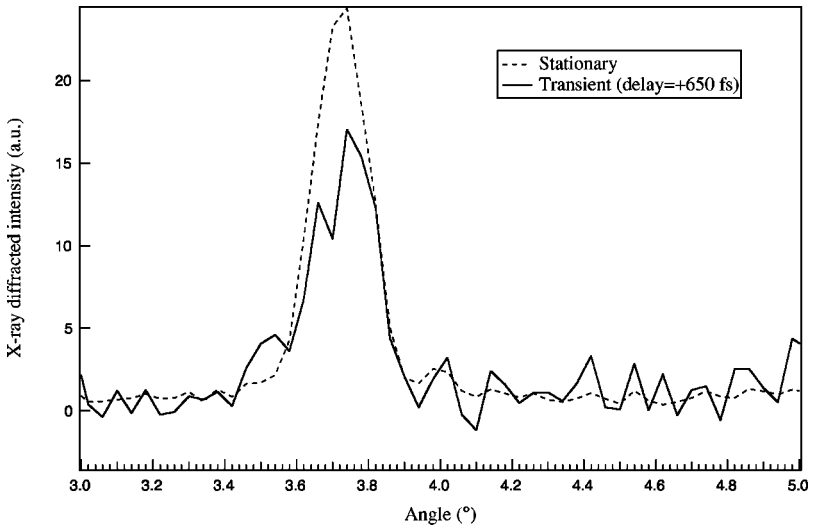

FIG. 8. Experimental stationary and transient rocking curves (measurements of the present authors at the Laboratoire d'Optique Appliquée).

et al., 1999). The difference is due to the fact that expansion of a sample a few hundred nanometers thick takes tens of picoseconds. The sudden change of temperature induced by the laser pulse means that the sample is no longer at its equilibrium density, but wishes to expand. This strain is relieved by a compression-expansion wave travelling from the surface at the speed of sound (Thomsen *et al.*, 1986). For a soft material such as the organic film the speed of sound is not more than 3 nm/ps, so in order to expand a significant fraction of the 230-nm-thick sample, several tens of picoseconds are needed. Before this has time to occur in our experiments, the heating induces local disorder that strongly diminishes the diffraction. We calculate the decrease $\delta(t)$ in diffracted intensity by normalizing the rocking curve $R(t,\theta)$ with the stationary value $R_0(\theta)$:

$$\delta(t)=\sum_{\theta} R_0(\theta)[R_0(\theta)-R(t,\theta)]. \tag{1}$$

The decrease is then divided by the value $\delta(\infty)$ measured long time after the shot, in order to compensate for the fact that the heating pulse does not cover the x-ray focus completely. The disorder induced in the cadmium layers results in a broadening of the electron distribution. Quantitatively, we may take the distribution $f(z)$ to be a Gaussian function of the distance z to the center of the layer,

$$f(z)\propto \frac{1}{\sigma(t)}\exp[-z^2/2\sigma(t)^2], \tag{2}$$

where $\sigma(t)$ is the half-width of the distribution. The intensity of the Bragg peak is then well approximated by

$$I(t)=I_0\exp[-2\pi\sigma(t)^2/d^2], \tag{3}$$

where d is the distance between the cadmium layers (55 Å) and I_0 is the intensity for $\sigma=0$. For the cold film σ equals 1.5 Å, which gives $I=0.97I_0$. The intensity is seen to drop to $I_0/e=0.37I_0$ when $\sigma(t)$ reaches $d/2\pi=8.8$ Å. The observed decrease in diffracted intensity is shown as function of time in Fig. 9 for the two different intensities of the heating pulse. The time required for broadening of the cadmium layers is seen to differ by more than one order of magnitude. This response time is affected by several quantities: (i) The time required to transfer energy from the photons into motion of the atoms. (ii) The velocity acquired by the cadmium atoms. (iii) The mobility of the cadmium atoms, determined by the "viscosity" of the superheated film. All three can be expected to be nonlinear functions of the heating energy, so the

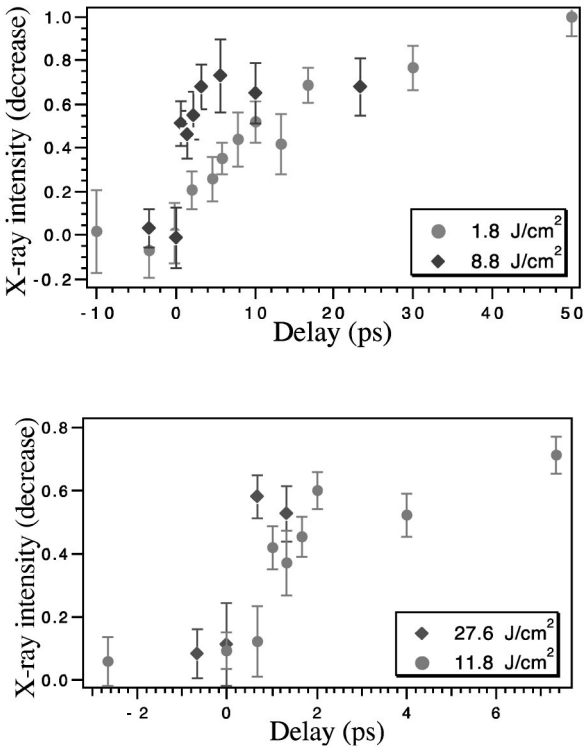

FIG. 9. Decrease (plotted in the figure as an increase of the signal) in diffracted intensity as a function of time. Negative delays correspond to the response of the unperturbed sample.

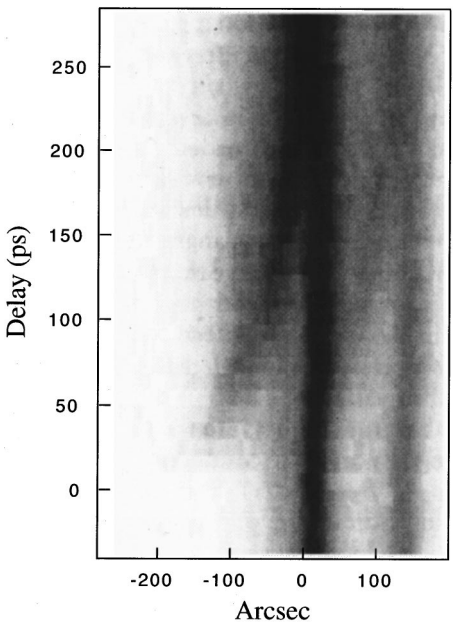

FIG. 10. X-ray diffracted lines ($K_{\alpha 1}$ and $K_{\alpha 2}$) as a function of the delay in the UCSD experiment (Rose-Petruck *et al.*, 1999).

strong sensitivity to the pulse intensity is not surprising. Numerical simulations are required to investigate these different processes quantitatively. In the case of high pump energy, the diffraction is seen not to disappear completely within the time window of the experiment. This behavior probably arises from the incomplete coverage of the x-ray focus of the heating pulse, due to the narrow focusing necessary to attain high energies. A part of the x-ray focus is exposed to the edge of the heating beam where the intensity is lower, and this adds components with slower response times to the signal.

C. Other experiments

The first experiments presented above are mainly demonstrations of the technique, but the field is presently moving towards real applications in solid-state physics. Three other groups (one at the University of California San Diego and two at the ALS) have published results with picosecond time resolution (Chin *et al.*, 1999; Siders *et al.*, 1999; Rose-Petruck *et al.*, 1999; Lindenberg *et al.*, 2000). Direct observation of coherent acoustic motions in a GaAs crystal using a laser-produced plasma x-ray source has been reported by Rose-Petruck and co-workers at UCSD (1999). Milliångström changes in lattice spacing were measured with picosecond temporal resolution. The optical energy is transfered to the lattice within a few picoseconds through the production of longitudinal optical phonons which decay into acoustic phonons. The thermal stress generated at the crystal surface is relieved by lattice expansion, starting at the surface, and a travelling compression-expansion wave is launched into the crystal. Figure 10 shows the experimentally measured x-ray-diffraction curves as a function of the Bragg angle and the delay following the optical excitation. At early times,

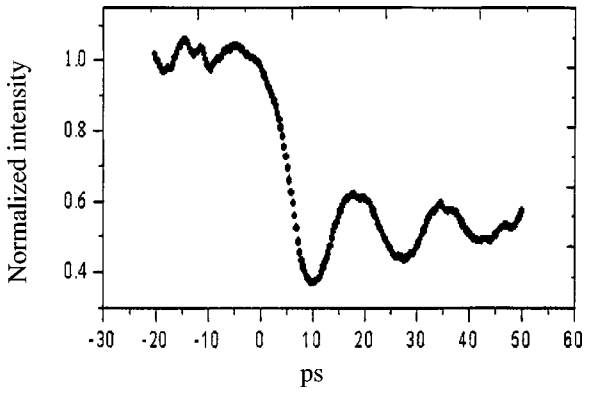

FIG. 11. X-ray transient signal from streak camera experiments at Berkeley (Lindenberg *et al.*, 2000).

the broad x-ray diffracted line reflects the expansion of the very top layers while for longer delays, the strain propagates away from the surface, leading to a negative (expansion) and a slight positive shift (compression) of the line.

Experiments using fast x-ray streak cameras with a resolution of 2 ps have also been reported by Falcone and co-workers at Berkeley (Larsson *et al.*, 1997, 1998; Lindenberg *et al.*, 2000). The most impressive result is the first observation of the temporal oscillations in the x-ray intensity produced by the coherent lattice oscillations. Figure 11 shows the time-resolved x-ray diffracted intensity as a function of the time following the excitation of an InSb sample at a fluence of 15 mJ/cm^2, 20% lower than the damage threshold of the lattice. They interpret these results as arising from coherent acoustic oscillations excited by the ultrafast heating of the lattice. At slightly higher fluences, they detect a reversible order-disorder transition phase, driven by large amplitude, coherent vibrational motion.

V. CONCLUSIONS

For many years, subpicosecond x-ray diffraction was one of the holy grails of ultrafast science. In this paper we have reviewed how this goal was reached and discussed some of the exciting future applications in biology and solid-state physics. Progress has depended on the development of new x-ray sources and detection schemes, with laser-produced plasma sources and synchrotron radiation detected by streak cameras emerging as the methods of choice. We believe that these two technologies will remain the most important for the next several years, essentially in their present forms. The femtosecond synchrotron source at the ALS may provide complementary possibilities.

The most recent experimental results show that the present technical capabilities permit great advances in the understanding of the response of solids to impulsive heating. We expect that in the next few years, phenomena such as ultrafast melting, ordinary laser-induced melting and propagation of strain waves will be characterized in detail. Beyond this stage awaits the challenge

of detecting many different reflections in order to reconstruct the directions of atomic motions—in other words, the development of true femtosecond crystallography.

ACKNOWLEDGMENTS

The femtosecond x-ray-diffraction project at the Laboratoire d'Optique Appliquée is a fruitful collaboration with I. Uschmann and E. Förster, University of Jena, J.-P. Geindre, and P. Audebert, Ecole Polytechnique, and P.-A. Albouy, Université d'Orsay. We gratefully acknowledge the support of the laser staff at the LOA. We acknowledge very helpful discussions with G. Lompré and I. Nenner from Commissariat à l'Energie Atomique, J. L. Martin from LOA, and K. Scheidt, G. Naylor, and M. Wulff from ESRF. This work was supported by the Center National de la Recherche Scientifique, the European Community Commission under the Large Facilities Contract No. CHGE-CT93-0021, under the Human Capital and Mobility Contract No. CHRX-CT93-0338, and Training and Mobility Contract No. CHRX-CT96-0080.

REFERENCES

Afonso, C. N., J. Solis, F. Catalina, and C. Kalpouzos, 1996, Appl. Phys. Lett. **76**, 2519.

Backus, S., C. G. Durfee III, M. M. Murmane, and H. C. Kapteyn, 1998, Rev. Sci. Instrum. **69**, 1207.

Baltuska, A., Z. Wei, M. S. Pshenichnikov, and D. A. Wiersma, 1997, Opt. Lett. **22**, 102.

Bastiani, S., A. Rousse, J. P. Geindre, P. Audebert, C. Quoix, G. Hamoniaux, A. Antonetti, and J. C. Gauthier, 1997, Phys. Rev. E **56**, 7179.

Brabec, T., and F. Krausz, 2000, Rev. Mod. Phys. **72**, 545.

Bucksbaum, P. H., and R. Merlin, 1999, Solid State Commun. **111**, 535.

Cao, J. M., H. Ihee, and A. H. Zewail, 1999, Proc. Natl. Acad. Sci. USA **96**, 338.

Cao, J. S., and K. R. Wilson, 1999, J. Phys. Chem. A **102**, 9523.

Chambaret, J. P., C. LeBlanc, G. Cheriaux, P. Curley, G. Darpentigny, P. Rousseau, G. Hamoniaux, A. Antonetti, and F. Salin, 1996, Opt. Lett. **21**, 1921.

Chan, K. C. D., G. P. Lawrence, and J. D. Schneider, 1998, Nucl. Instrum. Methods Phys. Res. B **139**, 394.

Chang, Z., A. Rundquist, J. Zhou, M. M. Murnane, H. C. Kapteyn, X. Liu, B. Shan, J. Liu, L. Niu, M. Gong, and X. Zhang, 1996, Appl. Phys. Lett. **60**, 133.

Chen, P., V. Tomov, and P. M. Rentzepis, 1996, J. Chem. Phys. **104**, 10001.

Chin, A. H., R. W. Schoenlein, T. E. Glover, P. Balling, W. P. Leemans, and C. V. Shank, 1999, Phys. Rev. Lett. **83**, 336.

Dougherty, T. P., G. P. Wiederrecht, K. A. Nelson, M. H. Garrett, H. P. Jensen, and C. Warde, 1992, Science **258**, 770.

Edman, K., P. Nollert, A. Royant, H. Belrhali, E. Pebay-Peyroula, J. Hadju, R. Neutze, and E. M. Landau, 1999, Nature (London) **401**, 822.

Esarey, E., P. Sprangle, J. Kralland, and A. Ting, 1996, IEEE Trans. Plasma Sci. **24**, 252.

Fann, W. S., R. Storz, H. W. K. Tom, and J. Bokor, 1992, Phys. Rev. B **46**, 13592.

Franzen, S., B. Bohn, C. Poyart, and J.-L. Martin, 1995, Biochemistry **34**, 1224.

Gai, F., K. C. Hasson, J. C. McDonald, and P. A. Anfinrud, 1998, Science **279**, 1886.

Galdecka, E., 1995, in *International Tables for Crystallography*, edited by A. J. C. Wilson (Kluwer, Dordrecht/Boston/London), p. 434.

Gauthier, J. C., S. Bastiani, P. Audebert, J. P. Geindre, A. Rousse, C. Quoix, G. Grillon, A. Mysyrowicz, A. Antonetti, R. Mancini, and A. Shlyaptseva, 1997, in *Proceedings of the SPIE*, San Diego, edited by G. A. Kyrala and J. C. Gauthier (SPIE, San Diego), Vol. 3157, pp. 52–63.

Gauthier, J. C., J. P. Geindre, P. Audebert, S. Bastiani, C. Quoix, G. Grillon, A. Mysyrowicz, A. Antonetti, and R. C. Mancini, 1997, Phys. Plasmas **4**, 1811.

Glezer, E. N., Y. Siegal, L. Huang, and E. Mazur, 1995a, Phys. Rev. B **51**, 6959.

Glezer, E. N., Y. Siegal, L. Huang, and E. Mazur, 1995b, Phys. Rev. B **51**, 9589.

Graves, J. S., and R. E. Allen, 1999, Phys. Rev. B **58**, 13627.

Guo, T., C. Rose-Petruck, R. Jimenez, F. Ràski, J. A. Squier, B. C. Walker, K. Wilson, and C. P. J. Barty, 1997, in *Proceedings of the SPIE*, San Diego, edited by A. Kyrala and J. C. Gauthier (SPIE, San Diego), Vol. 3157, pp. 84–92.

Hartmann, H., S. Zinser, P. Komninos, R. T. Schneider, G. U. Nienhaus, and F. Parak, 1996, Proc. Natl. Acad. Sci. USA **93**, 7013.

Helliwell, J. R., and P. M. Rentzepis, 1997, *Time-resolved Diffraction* (Clarendon Press, Oxford).

Huang, L., J. P. Callan, E. N. Glezer, and E. Mazur, 1998, Phys. Rev. Lett. **80**, 185.

Jona, F., and G. Chirane, 1962, *Ferroelectric Crystals* (Pergamon Press, Oxford).

Kieffer, J. C., M. Chaker, J.-P. Matte, H. Pepin, C.-Y. Cote, Y. Beaudoin, T. W. Johnston, C.-Y. Chien, S. Coe, G. Mourou, and O. Peyrusse, 1993, Phys. Fluids B **5**, 2676.

Kieffer, J.-C., Z. Jiang, A. Ikhlef, and C. Y. J. Côté, 1996, J. Opt. Soc. Am. B **13**, 132.

Kochendoerfer, G. G., and R. A. Mathies, 1995, Isr. J. Chem. **35**, 211.

Lanyi, J. K., 1997, J. Biol. Chem. **272**, 31209.

Larson, B. C., C. W. White, T. S. Noggle, J. F. Barhorst, and D. M. Mills, 1982, Phys. Rev. Lett. **48**, 337.

Larson, B. C., C. W. White, T. S. Noggle, J. F. Barhorst, and D. M. Mills, 1983, Appl. Phys. Lett. **42**, 282.

Larsson, J., Z. Chang, E. Judd, P. J. Schuck, R. W. Falcone, P. A. Heimann, H. A. Padmore, H. C. Kapteyn, P. H. Bucksbaum, M. M. Murnane, R. W. Lee, A. Machacek, J. S. Wark, X. Liu, and B. Shan, 1997, Opt. Lett. **22**, 1012.

Larsson, J., P. A. Heimann, A. M. Lindenberg, P. J. Schuck, P. H. Bucksbaum, R. W. Lee, H. A. Padmore, J. S. Wark, and R. W. Falcone, 1998, Appl. Phys. A: Mater. Sci. Process. **66**, 587.

Liebl, U., J. C. Lambry, W. Leibl, J. Breton, J. L. Martin, and M. H. Vos, 1996, Biochemistry **35**, 9925.

Lindenberg, A. M., I. Kang, S. L. Johnson, T. Missalla, P. A. Heimann, Z. Chang, J. Larsson, P. H. Bucksbaum, H. C. Kapteyn, H. A. Padmore, R. W. Lee, J. S. Wark, and R. W. Falcone, 2000, Phys. Rev. Lett. **84**, 111.

Lindl, J., 1995, Phys. Plasmas **2**, 3933.

Lunney, J. G., P. J. Dobson, J. D. Hares, S. D. Tabatabaei, and R. W. Eason, 1986, Opt. Commun. **58**, 269.

Makinen, M. W., and W. A. Eaton, 1973, Ann. (N.Y.) Acad. Sci. **206**, 210.
Modena, A., Z. Najmudin, A. E. Dangor, C. E. Clayton, K. A. Marsh, C. Joshi, V. Malka, C. B. Darrow, C. Danson, D. Neely, and F. N. Walsh, 1995, Nature (London) **377**, 606.
Mourou, G., C. P. Barty, and M. Perry, 1998, Phys. Today **51**(1), 22.
Murnane, M. M., H. C. Kapteyn, M. D. Rosen, and R. W. Falcone, 1991, Science **251**, 531.
Neutze, R., and J. Hadju, 1997, Proc. Natl. Acad. Sci. USA **94**, 5651.
Nienhaus, G. U., J. D. Müller, B. H. McMahon, and H. Frauenfelder, 1997, Physica D **107**, 297.
Othonos, A., 1998, J. Appl. Phys. **83**, 1789.
Perman, B., V. Šřajer, Z. Ren, T. Y. Teng, C. Pradervand, T. Ursby, D. Bourgeois, F. Schotte, M. Wulff, R. Kort, K. Hellingwerf, and K. Moffat, 1998, Science **279**, 1946.
Perry, M. D., and G. Mourou, 1994, Science **264**, 917.
Perutz, M. F., A. J. Wilkinson, M. Paoli, and G. G. Dodson, 1998, Annu. Rev. Biophys. Biomol. Struct. **27**, 1.
Pronko, P. P., S. K. Dutta, J. Squier, J. V. Rudd, D. Duand, and G. Mourou, 1995, Opt. Commun. **114**, 106.
Rischel, C., A. Rousse, I. Uschmann, P. A. Albouy, J. P. Geindre, P. Audebert, J. C. Gauthier, E. Foerster, J. L. Martin, and A. Antonetti, 1997, Nature (London) **390**, 490.
Rose-Petruck, C., R. Jimenez, T. Guo, A. Cavalleri, C. W. Siders, F. Ràski, J. A. Squier, B. C. Walker, K. Wilson, and C. P. J. Barty, 1999, Nature (London) **398**, 310.
Rousse, A., P. Audebert, J. P. Geindre, F. Falliès, J. C. Gauthier, A. Mysyrowicz, G. Grillon, and A. Antonetti, 1994, Phys. Rev. E **50**, 2200.
Rousse, A., C. Rischel, I. Uschmann, P. A. Albouy, J. P. Geindre, P. Audebert, J. C. Gauthier, E. Förster, and A. Antonetti, 1999, J. Appl. Crystallogr. **32**, 977.
Saeta, P., J.-K. Wang, Y. Siegal, N. Bloembergen, and E. Mazur, 1991, Phys. Rev. Lett. **67**, 1023.
Schlichting, I., J. Berendzen, G. N. Phillips, and R. M. Sweet, 1994, Nature (London) **371**, 808.
Schoenlein, R. W., S. Chattopadhyay, H. H. W. Chong, T. E. Glover, P. A. Heimann, C. V. Shank, A. Zholents, and M. Zolotorev, 2000, Science **287**, 2237.
Schoenlein, R. W., W. P. Leemans, A. H. Chin, P. Volfbeyn, T. E. Glover, P. Balling, M. Zolotorev, K. J. Kim, S. Chattopadhyay, and C. V. Shank, 1996, Science **274**, 236.
Shank, C. V., R. Yen, and C. Hirlimann, 1983a, Phys. Rev. Lett. **51**, 900.
Shank, C. V., R. Yen and C. Hirlimann, 1983b, Phys. Rev. Lett. **50**, 454.
Shumay, I. L., and U. Höfer, 1996, Phys. Rev. B **53**, 15878.
Siders, C. W., A. Cavalleri, K. Sokolowski-Tinten, C. Toth, T. Guo, M. Kammler, M. H. v. Hoegen, K. R. Wilson, D. v. d. Linde, and C. P. J. Barty, 1999, Science **286**, 1340.
Sokoloff, J. P., L. L. Chase, and D. Rytz, 1988, Phys. Rev. B **38**, 597.
Sokolowski-Tinten, K., H. Schulz, J. Bialkowski, and D. von der Linde, 1991, Appl. Phys. A: Solids Surf. **53**, 227.
Sokolowski-Tinten, K., J. Bialkowski and D. von der Linde, 1995, Phys. Rev. B **51**, 14186.
Sokolowski-Tinten, K., J. Bialkowski, M. Boing, A. Cavalleri, and D. v. d. Linde, 1998, Phys. Rev. B **58**, R11805.
Solis, J., C. N. Afonso, S. C. W. Hyde, N. P. Barry, and P. M. W. French, 1996, Phys. Rev. Lett. **76**, 2519.
Solis, J., M. C. Morilla, and C. N. Afonso, 1998, J. Appl. Phys. **84**, 5543.
Šřajer, V., T. Teng, T. Ursby, C. Pradervand, Z. Ren, S. Adachi, W. Schildkamp, D. Bourgeois, M. Wulff, and K. Moffat, 1996, Science **274**, 1726.
Stampfli, P., and K. H. Bennemann, 1994, Phys. Rev. B **49**, 7299.
Stampfli, P., and K. H. Bennemann, 1995, Appl. Phys. A: Mater. Sci. Process. **60**, 191.
Stingl, A., M. Lenzner, C. Spielmann, F. Krausz, and R. Sipocs, 1995, Opt. Lett. **20**, 602.
Stuart, B. C., M. D. Feit, A. M. Rubenchik, B. W. Shore, and M. D. Perry, 1995, Phys. Rev. Lett. **74**, 2248.
Stuart, B. C., M. D. Feit, S. Herman, A. M. Rubenchik, B. W. Shore, and M. D. Perry, 1996, J. Opt. Soc. Am. B **13**, 459.
Stuart, B. C., M. D. Feit, A. M. Rubenchik, B. W. Shore, and M. D. Perry, 1996, Phys. Rev. B **53**, 1749.
Teng, T. Y., V. Šřajer, and K. Moffat, 1997, Biochemistry **36**, 12087.
Thomsen, C., H. T. Grahn, H. J. Maris, and J. Tauc, 1986, Phys. Rev. B **34**, 4129.
Tomov, I. V., P. Chen, S. H. Lin, and P. M. Rentzepis, 1997, in *Time-Resolved Diffraction*, edited by J. R. Helliwell and P. M. Rentzepis (Clarendon Press, Oxford), pp. 1–42.
Vos, M. H., J.-C. Lambry, S. J. Robles, D. C. Youvan, J. Breton, and J.-L. Martin, 1991, Proc. Natl. Acad. Sci. USA **88**, 8885.
Vos, M. H., F. Rappaport, J.-C. Lambry, J. Breton, and J.-L. Martin, 1993, Nature (London) **363**, 320.
Vos, M. H., and J.-L. Martin, 1999, BBA-Bioenergetics **1411**, 1.
Wark, J. S., N. C. Woolsey, and R. R. Whitlock, 1992, Appl. Phys. Lett. **61**, 651.
Wark, J., 1996, Contemp. Phys. **37**, 205.
Wiik, B. H., 1997, Nucl. Instrum. Methods Phys. Res. A **398**, 1.
Williamson, J. C., M. Dantus, S. B. Kim, and A. H. Zewail, 1992, Chem. Phys. Lett. **196**, 529.
Williamson, J. C., and A. H. Zewail, 1994, J. Phys. Chem. **98**, 2766.
Wulff, M., D. Bourgeois, T. Ursby, L. Goir, and G. Mourou, 1997, in *Time-Resolved Diffraction*, edited by J. R. Helliwell and P. M. Rentzepis (Clarendon Press, Oxford), pp. 195–228.
Wulff, M., D. Bourgeois, and F. Schotte, 1997, Highlights ESRF 1996/1997.
Zewail, A. H., 1996, J. Phys. Chem. **100**, 12701.
Zholents, A. A., and M. S. Zolotorev, 1996, Phys. Rev. Lett. **76**, 916.
Zigler, A., J. H. Undewood, J. Zhu, and R. W. Falcone, 1987, Appl. Phys. Lett. **51**, 1873.